THE JOURNAL OF BIOLOGICAL CHEMISTRY VOL. 285, NO. 34, pp. 26545–26557, August 20, 2010

NADPH Oxidases Regulate CD44 and Hyaluronic Acid Expression in Thrombin-treated Vascular Smooth Muscle Cells and in Atherosclerosis*

Received for publication, May 11, 2010, and in revised form, June 7, 2010 Published, JBC Papers in Press, June 17, 2010, DOI 10.1074/jbc.M110.143917

Aleksandr E. Vendrov[‡1], Nageswara R. Madamanchi[‡1], Xi-Lin Niu[‡], Kimberly C. Molnar[‡], Mason Runge[‡], Cédric Szyndralewiez[§], Patrick Page[§], and Marschall S. Runge[‡2]

From the [‡]Department of Medicine, McAllister Heart Institute, University of North Carolina, Chapel Hill, North Carolina 27599-7126 and [§]GenKyoTex S.A., 14 Chemin des Aulx, 1228 Plan-les-Ouates, Geneva, Switzerland

The intracellular signaling events by which NADPH oxidase-generated reactive oxygen species (ROS) modulate vascular smooth muscle cell (VSMC) function and atherogenesis are yet to be entirely elucidated. We previously demonstrated that NADPH oxidase deficiency decreased atherosclerosis in apoE$^{-/-}$ mice and identified adhesion protein CD44 as an important ROS-sensitive gene expressed in VSMC and atherosclerotic lesions. Here, we examined the molecular mechanisms by which NADPH oxidase-generated ROS regulate the expression of CD44 and its principal ligand, hyaluronan (HA), and how CD44-HA interaction affects VSMC proliferation and migration and inflammatory gene expression in apoE$^{-/-}$ mice aortas. Thrombin-induced CD44 expression is mediated by transcription factor AP-1 in a NADPH oxidase-dependent manner. NADPH oxidase-mediated ROS generation enhanced thrombin-induced HA synthesis, and hyaluronan synthase 2 expression in VSMC. Hyaluronidase, which generates low molecular weight HA (LMW-HA), is induced in VSMC in a NADPH oxidase-dependent manner and LMW-HA stimulated ROS generation and cell proliferation in wild-type but not p47$^{phox-/-}$ VSMC, effects that were enhanced by thrombin pretreatment. Haptotactic VSMC migration toward HA was increased by thrombin in a CD44-dependent manner. HA expression in atherosclerotic lesions and plasma-soluble CD44 and HA levels were higher in apoE$^{-/-}$ compared with apoE$^{-/-}$/p47$^{phox-/-}$ mice. HA-regulated pro-inflammatory gene expression was higher in apoE$^{-/-}$ than apoE$^{-/-}$/p47$^{phox-/-}$ mouse aortas. GKT136901, a specific inhibitor of Nox1- and Nox4-containing NADPH oxidase activity, attenuated ROS generation and atherosclerosis and decreased CD44 and HA expression in atherosclerotic lesions. Together, these data suggest that increased CD44 and HA expression and CD44-HA-dependent gene regulation may play a role in atherosclerosis stimulated by NADPH oxidase activation.

Atherosclerosis is a chronic inflammatory disease of the vessel wall in which reactive oxygen species (ROS)[3]-mediated activation of redox-sensitive transcription pathways modulates atherosclerotic plaque progression. Increased adhesion molecule expression and remodeling of extracellular matrix are among the major changes caused by the activation of redox-sensitive signaling pathways. NADPH oxidases are critical determinants of the redox status of the vessel wall and play a critical role in the pathophysiology of atherosclerosis.

Several homologs of the gp91^{phox} (Nox2) catalytic moiety of multisubunit NADPH oxidase (Nox): Nox1, Nox3, Nox4, Nox5, Duox1 and Duox2, have been recently identified (1). All Nox homologs are transmembrane proteins that possess six transmembrane domains with conserved binding sites for FAD and NADPH and four heme-binding histidines in the third and fifth transmembrane domains. The Nox moieties have distinct subcellular localizations (2) and are differentially regulated. For the Nox2-containing NADPH oxidase, catalytic activity is initiated following assembly of cytosolic subunits p47^{phox} and p67^{phox} with the membrane-bound Nox2, a process that requires phosphorylation of p47^{phox} and p67^{phox}, protein-protein interaction, and binding of G protein Rac (1). In the case of Nox1 and Nox3-based NADPH oxidases, the cytosolic subunits p47^{phox} and p67^{phox} are replaced by Nox organizer 1 and Nox activator 1, respectively. The activation of Nox4 does not require any of the cytosolic subunits mentioned above. However, Lyle *et al.* (3) recently reported that polymerase Δ-interacting protein 2 associates with p22^{phox} to activate Nox4-based NADPH oxidase. Nox1- and Nox4-based enzymes are the predominant NADPH oxidases in mouse vascular smooth muscle cells (VSMC).

CD44 is a major cell surface adhesion molecule expressed on many vascular cell types including leukocytes, macrophages, endothelial cells, and VSMC. The expression of CD44 is regulated in a NADPH oxidase-dependent manner (4). In its extra-

* This work was supported, in whole or in part, by National Institutes of Health Grants HL-57352 and AG 024282.

[1] Both authors contributed equally to this work.

[2] To whom correspondence should be addressed: 125 MacNider Hall, University of North Carolina, Chapel Hill, NC 27599-7005. Tel.: 919-843-6485; Fax: 919-843-5945; E-mail: mrunge@med.unc.edu.

[3] The abbreviations used are: ROS, reactive oxygen species; VSMC, vascular smooth muscle cells; HA, hyaluronic acid; *Has2*, hyaluronan synthase 2; *Hyal3*, hyaluronidase 3; LMW-HA, low-molecular weight HA; HMW-HA, high-molecular weight HA; DMNQ, 2,3-dimethoxy-1,4-naphthoquinone; GKT136901, 2-(2-chlorophenyl)-4-methyl-5-(pyridin-2-yl-methyl)-1*H*-pyrazolo[4,3-c]pyridine-3,6(2H,5H)-dione); HABP, HA-binding protein; HASMC, human aortic smooth muscle cell; PBD, p21 binding domain; DHE, dihydroethidium; IGF-1, insulin-like growth factor 1; PAK-1, p21-activated protein kinase 1; MCP-1, monocyte chemoattractant protein-1; DCFDA, 2′,7′-dichlorofluorescin diacetate.

cellular domain, CD44 contains hyaluronan-binding site through which it anchors hyaluronic acid (HA) to the cell surface. The binding of HA to CD44 has been shown to regulate cell activation, proliferation, migration, signal transduction, and gene expression (5).

Consistent with its pleiotropic function, altered expression or dysfunction of CD44 has been proposed to be contributory in several pathological conditions. CD44 expression is up-regulated in mouse and human atherosclerotic lesions (4, 6–8) and in neointimal VSMC after arterial injury (4, 9). CD44-deficient apoE$^{-/-}$ mice develop markedly decreased atherosclerosis as compared with wild-type apoE$^{-/-}$ littermates (6). Proteolytic cleavage of the CD44 extracellular domain from the cell surface by metalloproteases generates soluble CD44, and circulating soluble CD44 levels are increased in humans with various inflammatory diseases and malignancies (10, 11). To date, a direct association between circulating soluble CD44 levels and human atherosclerosis has not been clearly established (12).

HA, a major glycosaminoglycan constituent of the extracellular matrix, is the principal ligand of CD44. HA also binds to other cell surface receptors such as RHAMM (receptor for HA-mediated motility) and LYVE-1 (lymphatic vessel endothelial HA receptor). HA polymers range in sizes and have wide ranging and sometimes opposing biological function depending on the size (13). Interaction of HA with cell surface receptors and a variety of hyaladherins such as link protein, versican, and tumor necrosis factor-induced gene-6 can result in the formation of extracellular matrix that makes up the microenvironment of VSMC (14).

HA is synthesized on the cytoplasmic surface of the plasma membrane by integral glycosyl transferases and is exported directly into the extracellular space (15). There are three distinct HA synthase genes (*Has1*, *Has2*, and *Has3*) in mammals. HAS2 is the major HAS isoform in VSMC (16). Constant HA turnover occurs under normal physiologic conditions and the increase in HA levels during pathophysiologic conditions reflects the balance between its synthesis and catabolism. Hyaluronidase is the enzyme that degrades HA and two distinct hyaluronidase genes (*Hyal1* and *Hyal2*) have been reported to be involved in the intracellular and extracellular catabolism of HA in a CD44-dependent manner (17). In addition, ROS can degrade HA under oxidative conditions (18).

Because of its interaction with cell surface receptors, HA affects cell behavior through direct receptor-mediated effects on gene expression (19). Alterations in HA metabolism, distribution, and function have been documented in many diseases (14). HA was shown to regulate VSMC proliferation and activation *in vitro* (6) and overexpression of HA in aortic VSMC of apoE$^{-/-}$ mice has been shown to promote atherosclerosis development (20). Increased HA levels have been observed in injured rat carotid arteries and human restenotic arteries and atherosclerotic lesions (21, 22). Increased HA synthesis by saphenous vein VSMC is thought to contribute to saphenous vein graft failure in bypass patients (23) and selective accumulation of HA is associated with the proliferation and migration of VSMC and thrombosis of eroded plaques (22).

In the present study, we investigated the role of NADPH oxidases in thrombin-induced regulation of CD44 and HA expression in mouse VSMC and atherosclerosis. Our results demonstrate that NADPH oxidase plays a critical role in the regulation of both CD44 and HA expression in VSMC treated with thrombin. Low molecular weight HA (LMW-HA) enhances thrombin-induced NADPH oxidase activity and proliferation of VSMC, and HA-induced VSMC proliferation is regulated in a CD44-dependent manner. Absence of NADPH oxidase results in decreased levels of HA in the atherosclerotic lesions and soluble CD44 in the plasma and inflammatory gene expression in the aortic wall of apoE$^{-/-}$ mice. Additionally, our data suggest that Nox1- and Nox4-based NADPH oxidase inhibitors attenuate CD44 and HA expression in human aortic SMC and apoE$^{-/-}$ mice and decrease oxidative stress and atherosclerosis in the aortas of apoE$^{-/-}$ mice.

EXPERIMENTAL PROCEDURES

Chemicals and Reagents—If not stated otherwise, all chemicals were obtained from Sigma. 2,3-Dimethoxy-1,4-naphthoquinone (DMNQ) was purchased from Calbiochem. LMW-HA fragments were generated by sonication (24). Human α-thrombin was purchased from Hematologic Technologies, Inc. Rabbit anti-CD44 antibody and goat anti-HAS2 antibody were purchased from Santa Cruz Biotechnology. Mouse anti-β-actin antibody was obtained from Sigma. [^{3}H]Thymidine and UDP-[^{14}C]glucuronic acid were from PerkinElmer Life Sciences. GKT136901 (2-(2-chlorophenyl)-4-methyl-5-(pyridin-2-yl-methyl)-1*H*-pyrazolo[4,3-c]pyridine-3,6(2H,5H)-dione), a small molecule dual Nox1/Nox4 inhibitor (25) was provided by GenKyoTex S.A, and prepared in 0.5% carboxymethylcellulose, 0.25% Tween 20, 1% dimethyl sulfoxide. Luciferase reporter construct containing the human CD44 promoter fragment with regular or mutated AP-1 binding site were generously provided by Dr. Ashok Kumar, University of Ottawa (26).

Cell Culture—VSMC were isolated from aortas of 4-month-old wild-type, p47$^{phox-/-}$ and CD44$^{-/-}$ C57BL/6 mice as previously described (27). Aortas were dissected and digested with collagenase to remove adventitia and endothelium and then digested with collagenase and elastase at 37 °C for 1 h. VSMC were grown in Dulbecco's modified Eagle's medium (DMEM) containing 10% (v/v) fetal bovine serum (FBS) as previously described (28). Human aortic smooth muscle cells (HASMC) were purchased from Invitrogen and grown in smooth muscle basal medium supplemented with growth factors (SmGM-2, Lonza). All experiments were conducted using VSMC between passages 4 and 11 that were growth arrested by incubation in DMEM containing 0.1% FBS for 72 h.

Mice and Diet—Wild-type, p47$^{phox-/-}$, CD44$^{-/-}$, apoE$^{-/-}$, and apoE$^{-/-}$/p47$^{phox-/-}$ mice were bred in-house as previously described (29). All mice were on C57BL/6 genetic background. p47$^{phox-/-}$ and CD44$^{-/-}$ mice were backcrossed for 10 generations. Animals were maintained at 22 °C with a 12-h light/dark cycle and were fed standard rodent chow until 7–8 weeks of age and then a Western diet (42% fat, Harlan Teklad/TD88137) for 12 more weeks. GKT136901, at a concentration of 10 mg/kg of body weight, was delivered through oral gavage using 20-gauge gavage needles once daily and 5 days a week for 12 weeks. All procedures involving the experimental animals were performed in compliance with protocols approved by

University of North Carolina IACUC according to NIH guidelines.

AP-1 Transcription Factor Activity—Nuclear extracts from thrombin- and vehicle-treated VSMC were prepared with the NucBuster Protein Extraction Kit (Novagen) according to the manufacturer's protocol. AP-1 DNA binding activity was measured using the TransBinding AP-1 Assay Kit (Panomics). Briefly, nuclear extracts were incubated with biotinylated AP-1-consensus binding sequence oligonucleotides and the complexes bound to the oligonucleotides were detected using a primary AP-1 antibody and a secondary antibody conjugated to horseradish peroxidase. AP-1 activity was assayed by measuring the absorbance at 450 nm.

Nuclear Run-on Assay—Nuclei from thrombin-, DMNQ-, and vehicle-treated VSMC were isolated by lysing cells in 250 μl of lysis buffer (10 mM NaCl, 3 mM $MgCl_2$, 10 mM Tris-HCl, 0.5% Nonidet P-40, pH 7.4) and then resuspended in nuclei storage buffer (40% glycerol, 50 mM Tris-HCl, 5 mM $MgCl_2$, 0.1 mM EDTA, pH 8.5). Run-on transcription was done at room temperature for 30 min in a 100-μl volume with 2× reaction mixture containing 4× reaction buffer (100 mM HEPES, 10 mM $MgCl_2$, 10 mM DTT, 300 mM KCl, 20% glycerol), 1 mM NTPs, and 250 μCi of [α-^{32}P]UTP. Reactions were stopped by the addition of 2 units of DNase I at 37 °C for 10 min followed by incubation with 300 μl of stop buffer (2% SDS, 7 M urea, 0.35 M NaCl, 1 mM EDTA, 10 mM Tris-HCl, pH 8.0) and 15 μl of proteinase K (Qiagen) at 45 °C for 2 h. Dot blots containing 10 μg of denaturated CD44 and 18 S cDNAs were hybridized with nuclear run-on products in 5 ml of QuikHyb Hybridization Solution (Stratagene) at 42 °C for 24 h. The membranes were washed twice for 15 min at room temperature with 2× SSC, 0.1% SDS and then once for 30 min at 60 °C with 0.1× SSC, 0.1% SDS. Blots were analyzed by autoradiography.

RNA Extraction and Real Time RT-PCR—Total RNA from untreated and thrombin-treated wild-type and $p47^{phox-/-}$ cells was extracted using the RNeasy Micro Kit (Qiagen). RNA from mouse aortas was extracted with the MELT™ Total Nucleic Acid Isolation System (Ambion). Reverse transcription was performed with 1 μg of total RNA using a TaqMan Reverse Transcription Reagent kit (Applied Biosystems). TaqMan Gene Expression Assays for mouse *Cd44* (Mm01277161_m1), *Has2* (Mm00515089_m1), *Hyal3* (Mm00662097_m1), *Ccl2* (Mm00441242_m1), *Ccl4* (Mm00443111_m1), *Ccl5* (Mm01302428_m1), *Tnfα* (Mm00443258_m1), *Il1β* (Mm00434228_m1), *Igf1* (Mm00439560_m1) and for human *Cd44* (Hs01075861_m1), *Has2* (Hs00193435_m1), *Nox1* (Hs00246589_m1), and *Nox4* (Hs00418356_m1) were purchased from Applied Biosystems. Real time RT-PCR was carried out using the ABI PRISM 7900 HT Sequence Detection System and TaqMan PCR Master Mix according to the manufacturer's recommendations. Sequence Detection System software (Applied Biosystems) was used for raw data processing and analysis. The data for each gene were analyzed by REST2005 (Relative Expression Software Tool) (30). Relative expression of each gene was determined by normalization to 18 S ribosomal RNA expression.

Transient Transfection and Luciferase Activity Assay—VSMC were transfected with CD44 promoter luciferase reporter or pCMV-β-galactosidase constructs using the GenJet In Vitro DNA Transfection Kit for SMC (SignaGen Laboratories) as recommended by manufacturer. Cell suspensions were incubated for 20 min at 37 °C with 1 μg of CD44 promoter constructs and 0.5 μg of pCMV-β-galactosidase constructs mixed with 6 μl of GenJet reagent and serum-free DMEM. Fresh 10% FBS/DMEM was added to the mixture and cells were plated on 12-well plates. After 24 h, cells were quiesced in 0.1% FBS/DMEM for 72 h. Cells were treated with thrombin or vehicle for 8 h and lysed in GloLysis buffer (Promega). Cell lysate was mixed with either Bright-Glo luciferase substrate or Beta-Glo galactosidase substrate (Promega) in equal amounts. After a 10-min incubation, luminescence was measured using Wallac 1420 Multilabel plate reader.

Measurement of CD44 mRNA Stability—VSMC were treated with thrombin or vehicle for 4 h prior to the addition of actinomycin D (5 μg/ml). RNA was extracted at 0, 2, 4, and 6 h and analyzed with real time RT-PCR as described above.

Rac1 Activation Assay—Cell lysates from thrombin- and LMW-HA-treated VSMC were analyzed for Rac1 activation using the PAK-1 PBD pull-down method (Rac1 Activation Assay Kit, Millipore). This assay uses the Rac downstream effector, p21-activated protein kinase (PAK), to isolate the active GTP-bound form of Rac from the sample. The p21 binding domain (PBD) of PAK-1 is expressed as a GST fusion protein and coupled to agarose beads. Cell lysates were precleared with 100 μl of glutathione-agarose and then immunoprecipitated with 10 μg of PAK-1 PBD at 4 °C overnight. Agarose beads were washed and analyzed by Western blot using mouse anti-Rac1 antibody. Nonimmunoprecipitated lysates were analyzed by Western blot to adjust for protein loading.

Western Analysis—Western analysis was performed as described previously (28).

Intracellular ROS Detection—VSMC grown in glass-bottom plates were washed with Hanks' buffered salt solution and loaded with 10 μM H_2DCFDA (Invitrogen) in Hanks' buffered salt solution at 37 °C for 30 min and stimulated with Hanks' buffered salt solution containing 10 μM H_2DCFDA and either thrombin or LMW-HA. Fluorescence was read at 535 nm using Wallac 1420 Multilabel plate reader. VSMC treated with thrombin or LMW-HA were incubated with 10 μM dihydroethidium (DHE, Invitrogen) at 37 °C for 30 min. DHE fluorescence was obtained at 590 nm in several visual fields using a Leica DMIRB fluorescent microscope.

In Vitro Hyaluronan Synthase Activity Assay—VSMC were treated with thrombin or vehicle for 6 h and hyaluronan synthase (HAS) activity assay was performed as described previously (31). Cells were washed, incubated in lysis buffer (10 mM KCl, 1.5 mM $MgCl_2$, 10 mM Tris-HCl, pH 7.4) for 10 min, scraped, and homogenized using a Dounce homogenizer. Nuclei were removed by centrifuging at 1,000 × *g* for 4 min. Membrane fragments were separated by centrifugation at 16,000 × *g* for 25 min and resuspended in 100 μl of lysis buffer supplemented with protease inhibitors. HAS activity was determined in 100 μl of 25 mM HEPES (pH 7.1) containing 15 mM $MgCl_2$, 5 mM dithiothreitol, 0.2 μg of aprotinin, 5 μg of leupeptin, 1 mM UDP-GlcNAc, 50 μM UDP-GlcA, 0.25 μCi of UDP-[^{14}C]glucuronic acid, and 50 μg of cell membranes. The reac-

tion mixture was incubated at 37 °C for 1 h and terminated by boiling. The reaction mixtures were divided in two and treated with or without *Streptomyces* hyaluronate lyase at 37 °C overnight and then with 200 mg/ml of Pronase for 5 h. Deproteinized samples were centrifuged in Amicon Ultracell-100 Centrifugal Filters (Millipore) to remove unincorporated [^{14}C]glucuronic acid. Recovered samples were analyzed by liquid scintillation counting. HAS activity was calculated based on the incorporation rate of labeled glucuronic acid and as a fraction of HA removed by hyaluronate lyase treatment.

Histology and Immunostaining—The mouse hearts were perfused with PBS, embedded in OCT compound (Tissue-Tek), and snap-frozen in liquid nitrogen. Transverse serial sections were collected from the proximal aorta up to 560 μm of the cardiac tissue. Representative sections were stained with oil red O. Frozen sections were fixed in acetone and blocked with 0.3% H_2O_2 in methanol. Sections were immunostained with rat anti-mouse CD44 and CD11b antibodies (BD Pharmingen) or biotinylated HA-binding protein (Calbiochem) using the Vectastain Elite ABC Kit and Vector DAB Substrate Kit (Vector Laboratories). EPOS^{TM} Anti-human Smooth Muscle Actin/HRP antibody (DakoCytomation) was used with Vector DAB Substrate Kit (Vector Laboratories). VSMC were grown on chamber glass slides, treated with thrombin and hyaluronidase from *Streptomyces hyaluronlyticus* (Calbiochem). Cells were fixed in methanol at −20 °C for 10 min and in acetone at −20 °C for 1 min. Staining for HA was carried out using biotinylated HA-binding protein (HABP) with Vectastain Elite ABC Kit and Vector DAB Substrate Kit (Vector Laboratories). The numeric immunohistochemistry scoring (1, weak; 2, moderate; and 3, strong staining intensity) was performed by two independent observers blinded to the sample identity.

Haptotactic Cell Migration Assay—Cell migration assays were performed using 8-μm pore size Transwell chambers (Corning). The bottom side of the filters was coated with 100 μg/ml of HMW-HA or BSA. The filters were washed and blocked with 2% BSA in PBS. VSMC treated with vehicle or thrombin for 8 h were trypsinized, centrifuged, and resuspended in DMEM. Cells were incubated with 2 units/ml of thrombin, rat anti-mouse CD44 monoclonal antibody (Millipore), or normal mouse IgG (Santa Cruz Biotechnology) at 37 °C for 30 min, and 2×10^4 cells were seeded on the top of Transwell filters. Cells were incubated at 37 °C for 16 h. Transwells were washed with PBS, cells from the top side of the filter were removed with a cotton swab, and cells on the bottom side of the filter were stained with hematoxylin (Vector Laboratories). The number of stained cells in 10 × 10-mm grid was scored for six random fields (×20 objective) per Transwell filter. The average number of cells that migrated per filter was calculated.

[^{3}H]Thymidine Incorporation Assay—VSMC were plated at equal densities (2.5×10^4), quiesced, and either pretreated with thrombin for 8 h and then treated with LMW-HA for 24 h or treated with thrombin or LMW-HA for 24 h alone. [^{3}H]Thymidine (1 μCi/ml) was added for the last 4 h of treatment. Cells were then washed, treated with cold 5% trichloroacetic acid at 4 °C for 30 min, and lysed in 1 M sodium hydroxide. [^{3}H]Thymidine incorporation was determined by liquid scintillation counting.

Plasma Sample Collection and Hyaluronic Acid, Soluble CD44, and 8-Isoprostane ELISA—Blood samples were collected from deeply anesthetized mice through cardiac puncture and centrifuged at 1000 × *g* for 10 min for separation of plasma. Samples were stored at −80 °C until assayed. The concentration of HA in mouse plasma was measured using HA-ELISA (Echelon Biosciences) as described by the manufacturer. The Human CD44 ELISA kit (Cell Sciences) was used to measure soluble CD44 in mouse plasma and CD44 in protein lysates from mouse aortas. Plasma concentration of free 8-isoprostane was measured using the 8-isoprostane EIA Kit (Cayman Chemical) according to the manufacturer's protocol.

Statistical Analysis—Data were analyzed by one-way analysis of variance and post hoc analysis was performed using Newman-Keuls test. Student's *t* test was used to compare atherosclerosis, DHE fluorescence, 8-isoprostane levels, and immunohistochemistry scoring in mice treated with vehicle or GKT136901. Gene expression results in VSMC were analyzed by two-way analysis of variance followed by Bonferroni post-test. Differences were considered significant at $p < 0.05$.

RESULTS

Thrombin Induces Cd44 Expression in VSMC through NADPH Oxidase-dependent Activation of AP-1—We previously reported NADPH oxidase-dependent regulation of CD44 expression in wild-type VSMC treated with thrombin for 8 h (4). Consistent with these findings, a time-dependent activation of *Cd44* mRNA expression was observed in response to thrombin treatment in wild-type VSMC, but not in p47$^{phox-/-}$ VSMC (Fig. 1*A*). To determine whether differences in *Cd44* mRNA levels between wild-type and p47$^{phox-/-}$ VSMC were due to differences in gene transcription or mRNA stability, we first measured *de novo* transcription in nuclear run-on experiments. Thrombin treatment for 3 h resulted in a 2-fold increase in transcription of *Cd44* RNA ($p < 0.05$) in wild-type VSMC but had no significant effect in p47$^{phox-/-}$ cells (Fig. 1*B*). The thrombin-induced increase in CD44 mRNA expression was effectively blocked by pretreatment with diphenyleneiodonium chloride, an inhibitor of NADPH oxidases and other flavin-containing enzymes. Further support for redox-dependent regulation of *Cd44* mRNA expression was evident in wild-type VSMC treated with DMNQ, a redox cycling quinone known to induce ROS generation in VSMC (32).

Because the transcription factor AP-1 has been demonstrated to regulate CD44 expression during an inflammatory response in VSMC (33) and ROS have been implicated in the activation of AP-1 (34), we investigated activation of AP-1 in VSMC after treatment with thrombin. AP-1 DNA binding activity increased significantly (80%, $p < 0.05$) at 2 h and remained elevated for up to 4 h after thrombin treatment in wild-type but not in p47$^{phox-/-}$ cells (Fig. 1*C*). To determine whether NADPH oxidase-dependent increased AP-1 DNA binding activity is the mechanism for increased CD44 expression, wild-type and p47$^{phox-/-}$ VSMC were co-transfected with *Cd44* promoter-luciferase reporter gene constructs containing either an AP-1 binding sequence (from 5′ −334 to 3′

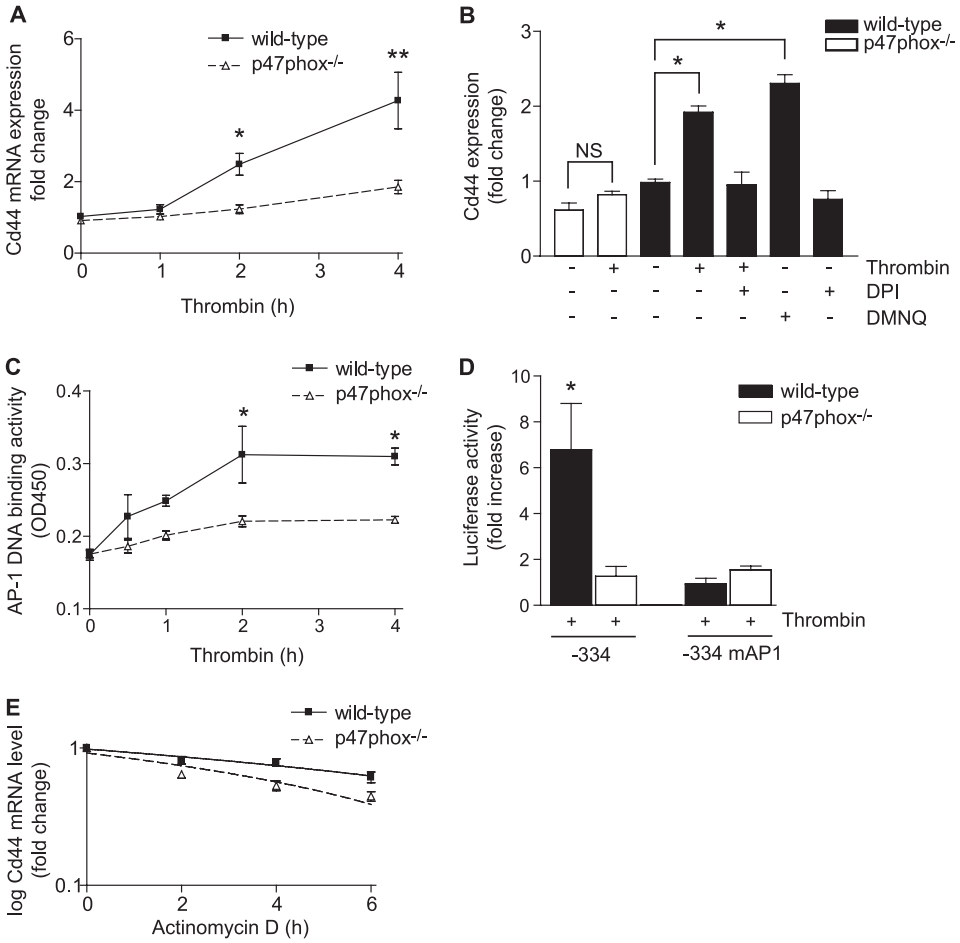

FIGURE 1. **NADPH oxidase-dependent activation of AP-1 regulates thrombin-induced *Cd44* gene expression.** *A,* real time RT-PCR analysis of *Cd44* expression in wild-type and p47$^{phox-/-}$ VSMC treated with thrombin. Data are expressed as fold-change in gene expression relative to untreated controls (mean ± S.E., $n = 3$, *, $p < 0.01$; **, $p < 0.001$). *B,* nuclear run-on analysis of *Cd44* transcription. Wild-type VSMC were pretreated with 20 μM diphenyleneiodonium chloride (*DPI*) for 30 min before treatment with 1 unit/ml of thrombin or 1 μM DMNQ for 3 h. p47$^{phox-/-}$ cells were treated with or without thrombin and nuclear extracts were analyzed by dot-blot. Densitometric analysis of *Cd44* mRNA expression, represented as fold-change, was calculated by first normalizing to 18 S RNA levels in individual samples and then relative to untreated wild-type control (mean ± S.E., $n = 3$, *, $p < 0.05$). *C,* DNA binding activity of AP-1 was assayed in wild-type and p47$^{phox-/-}$ VSMC after thrombin treatment. Data were expressed as absorbance at 450 nm (mean ± S.E., $n = 3$, *, $p < 0.05$, two-way analysis of variance). *D,* AP-1-dependent *Cd44* promoter activity was assayed in wild-type and p47$^{phox-/-}$ cells treated with thrombin. Cells were transiently co-transfected with *Cd44* promoter-luciferase constructs containing normal (*−334*) or mutated AP-1 (*−334 mAP-1*) binding sequences and β-galactosidase control plasmid. After 48 h, cells were treated with vehicle or thrombin for 6 h followed by luciferase and β-galactosidase activity measurement. Data represent fold-change in luciferase activity, normalized to β-galactosidase activity, in thrombin-treated cells compared with their respective controls (mean ± S.E., $n = 3$, *, $p < 0.05$). *E,* effect of thrombin on *Cd44* mRNA levels in the presence of actinomycin D. VSMC were pretreated with either vehicle or thrombin for 4 h and then treated with actinomycin D for the indicated times. *Cd44* RNA levels, assessed using real-time RT-PCR, were normalized to 18 S RNA levels. Data represent the fold-change in mRNA level relative to time 0 of actinomycin D addition (mean ± S.E., $n = 3$).

+53 bp containing gctgc**t**tag**t**ca) or a mutant AP-1 binding sequence (−334 mAP-1 containing gctgc**c**tag**g**ca) (26). The transfected cells were then treated with thrombin. Luciferase activities were 6.7-fold higher in thrombin-treated wild-type VSMC compared with untreated cells (Fig. 1*D*). Wild-type cells transfected with the mutant AP-1 CD44 promoter-luciferase reporter gene construct showed almost complete inhibition of luciferase activity in response to thrombin treatment compared with wild-type cells transfected with the control AP-1 CD44 promoter-luciferase reporter gene construct. Importantly, transfection of p47$^{phox-/-}$ VSMC with either control or the mutant AP-1 CD44 promoter-luciferase reporter gene construct failed to show any significant increase in luciferase activity compared with their respective controls (Fig. 1*D*).

We next investigated whether thrombin enhances the expression of CD44 by altering the stability of *Cd44* mRNA. The half-life of *Cd44* mRNA in control and thrombin-treated wild-type VSMC was assessed by mRNA chase experiments using the transcription inhibitor actinomycin D. *CdD44* mRNA stability was not altered by thrombin (Fig. 1*E*). Together, these results indicate that thrombin-induced CD44 expression in VSMC is regulated by AP-1 in NADPH oxidase-dependent manner.

Thrombin-induced HA Synthesis and Degradation in VSMC Are Regulated by NADPH Oxidase—A number of proatherogenic effects elicited by CD44 in vascular cells, including VSMC differentiation and activation (6), production of soluble inflammatory markers such as interleukin-12 (35), MCP-1 (36), iNOS (37), are largely mediated through the interaction of CD44 with HA (LMW-HA in particular). To determine whether activation of NADPH oxidase by thrombin has an effect on HA synthesis, we performed immunocytochemical analysis of wild-type and p47$^{phox-/-}$ VSMC treated with thrombin using HABP (Fig. 2*A*). Thrombin markedly increased HA synthesis in wild-type cells compared with p47$^{phox-/-}$ cells. Hyaluronidase treatment prior to immunostaining, to catabolize extracellular HA and thus demonstrate the specificity of HABP in recognizing HA, abrogated HA staining of both the cell types.

Hyaluronan synthase 2 (HAS2) is a major source of HA (38, 39). Quantitative RT-PCR analysis was used to determine whether the observed thrombin-induced increase in HA levels in wild-type VSMC resulted from increased synthesis. A time-dependent increase in *Has2* expression was observed in wild-type VSMC treated with thrombin (Fig. 2*B*). A 3.6-fold increase ($p < 0.01$) in *Has2* expression was observed in wild-type VSMC at 4 h after thrombin stimulation. Consistent with the putative role of NADPH oxidase in regulating HA levels, thrombin treatment had no significant effect on *Has2* expression in p47$^{phox-/-}$ VSMC. Thrombin also had no significant effect on *Has1* and *Has3* expression in either cell type (data not shown).

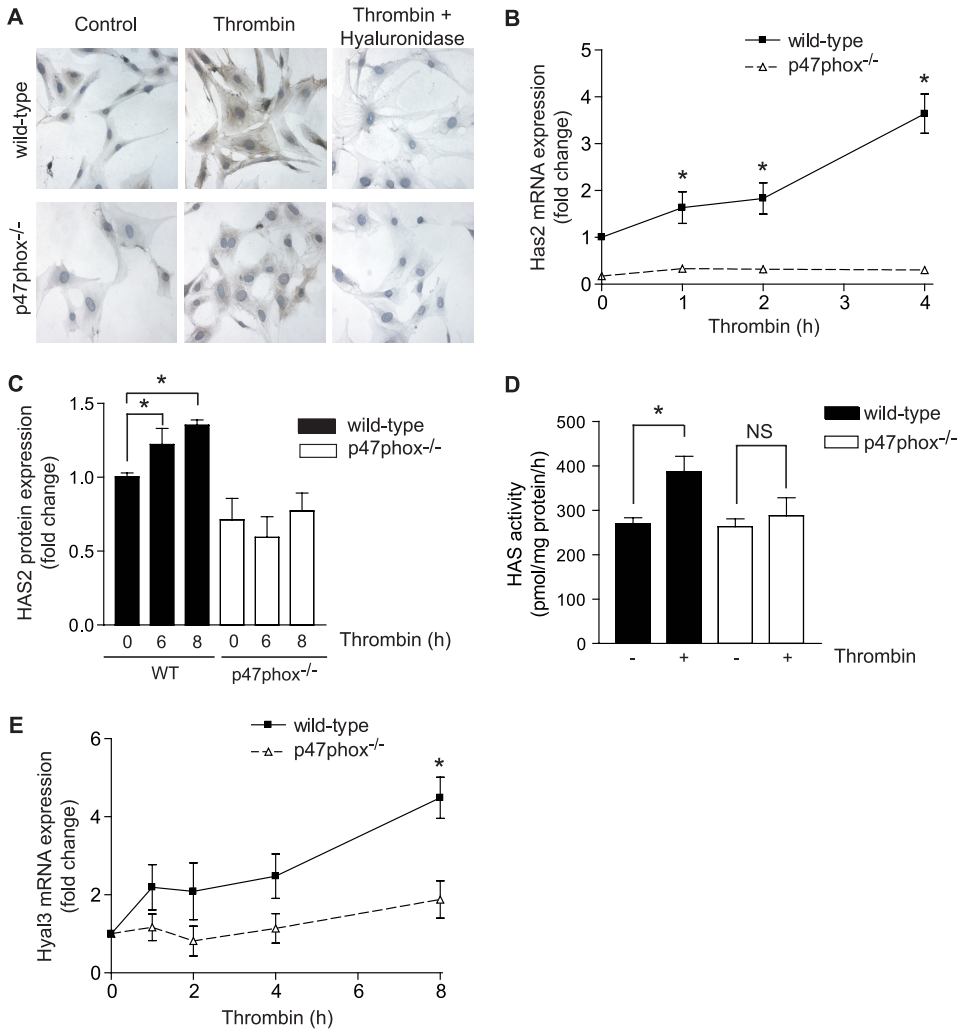

FIGURE 2. **NADPH oxidase regulates thrombin-induced increases in HAS2 and Hyal3 expression and HAS activity in VSMC.** *A,* VSMC were treated with thrombin for 24 h. HA was detected using biotinylated HABP. Pericellular localization of HA was shown by treatment with hyaluronidase for 30 min before staining with HABP. *B,* real time RT-PCR analysis of *Has2* RNA expression in VSMC treated with thrombin for the indicated times. Data represent fold-change in gene expression, normalized to 18 S RNA, and relative to untreated wild-type control (mean ± S.E., $n = 3$, *, $p < 0.001$). *C,* Western blot analysis of HAS2 protein levels in VSMC treated with thrombin. Densitometric analysis of protein levels, represented as fold-change, was calculated by first normalizing to β-actin levels in individual samples and then relative to untreated wild-type control (mean ± S.E., $n = 3$, *, $p < 0.05$). *D,* total HAS activity was measured in wild-type and p47$^{phox-/-}$ VSMC treated with thrombin or vehicle by analyzing UDP-[^{14}C]glucuronic acid incorporation rate. Data expressed as enzyme activity in picomole/h adjusted for total protein concentration (mean ± S.E., $n = 4$, *, $p < 0.05$, *NS*, not significant). *E,* real time RT-PCR analysis of *Hyal3* expression in VSMC treated with thrombin. Data expressed as fold-change in gene expression normalized to 18 S RNA and relative to untreated wild-type control (mean ± S.E., $n = 3$, *, $p < 0.05$).

Thrombin-induced increase in *Has2* mRNA levels was followed by a significant increase in the expression of HAS2 protein levels at 6 and 8 h in wild-type cells, but not in p47$^{phox-/-}$ cells (Fig. 2*C*). We then examined whether thrombin also regulates HAS activity in NADPH oxidase-dependent manner (Fig. *2D*). Thrombin increased HAS activity by 40% in wild-type VSMC after 6 h treatment ($p < 0.05$), whereas it had no significant effect on the activity of this enzyme in p47$^{phox-/-}$ cells (Fig. 2*D*). Interestingly, thrombin treatment also caused a time-dependent increase in the expression of hyaluronidase 3 (*Hyal3*) in wild-type, but not in p47$^{phox-/-}$ VSMC (Fig. 2*E*). *Hyal3* mRNA expression was 4.4-fold higher ($p < 0.01$) in wild-type VSMC than in p47$^{phox-/-}$ VSMC at 8 h after thrombin treatment. Thrombin had no significant effect on *Hyal1* and *Hyal2* expression in either cell type (data not shown). Taken together these data suggest that NADPH oxidase activation mediates thrombin-induced HA levels in VSMC by regulating both synthetic and degradation enzymes. Furthermore, ROS-regulated expression of *Hyal3* may lead to enhanced degradation of HA and generation of biologically active LMW-HA.

Interaction of Thrombin with LMW-HA Induces ROS Generation in NADPH Oxidase-dependent Manner via the Activation of Rac1—A sustained and marked increase in thrombin concentration occurs after arterial injury (40) and active thrombin has been shown to be present in human atherosclerotic lesions (41). Accumulation of HA has been observed in the plaque/thrombus interface in humans (22). Because these events likely involve NADPH oxidase activation, we investigated whether thrombin and LMW-HA interaction increases oxidative stress in VSMC. First, we quantified ROS production by measuring DCF fluorescence. Thrombin caused a 50% increase ($p < 0.05$) in DCF fluorescence in wild-type VSMC, but no significant increase in p47$^{phox-/-}$ VSMC (Fig. 3*A*). LMW-HA treatment significantly increased DCF fluorescence in wild-type ($p < 0.05$) but not in p47$^{phox-/-}$ cells. Wild-type VSMC pretreated with thrombin for 8 h and then treated with LMW-HA had 90% higher fluorescence compared with control cells ($p < 0.001$) and 30% higher fluorescence than thrombin-treated cells ($p < 0.05$) (Fig. 3*A*). Thrombin pretreatment followed by LMW-HA treatment had no significant effect on DCF fluorescence in p47$^{phox-/-}$ cells. Similar to its effect in wild-type cells, thrombin increased DCF fluorescence by 50% ($p < 0.05$) in CD44$^{-/-}$ VSMC (Fig. 3*A*). However, LMW-HA alone or pretreatment with thrombin followed by LMW-HA treatment had no significant effect on DCF fluorescence in CD44$^{-/-}$ VSMC, indicating that interaction of thrombin-induced CD44 with LMW-HA induces ROS generation in VSMC.

To confirm these results, we analyzed DHE fluorescence in wild-type, p47$^{phox-/-}$, and CD44$^{-/-}$ VSMC treated with thrombin, LMW-HA, or both. A marked increase in DHE fluorescence was observed in wild-type and CD44$^{-/-}$ VSMC treated with thrombin (data not shown). DHE fluorescence was

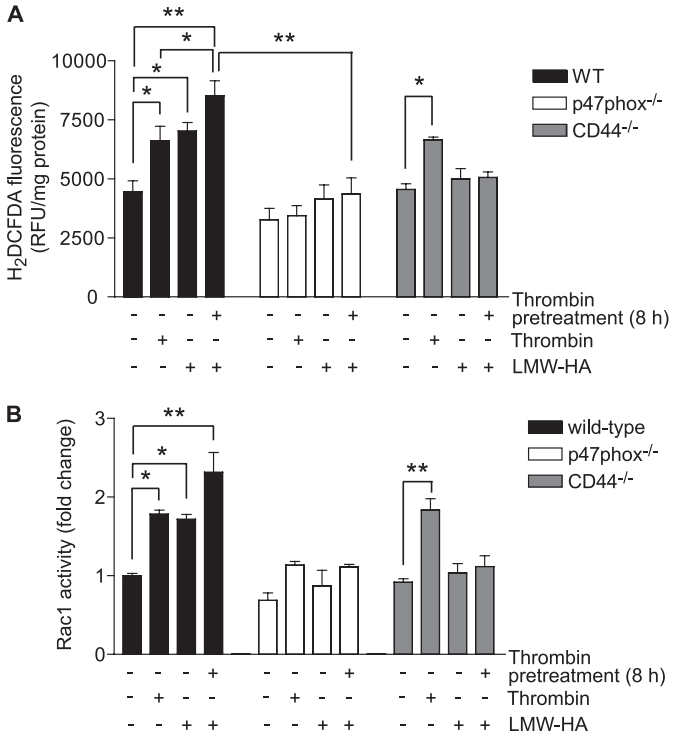

FIGURE 3. **Thrombin enhances LMW-HA-induced VSMC NADPH oxidase activity by enhancing Rac1 activity.** *A,* VSMC were treated with thrombin or LMW-HA alone or pretreated with thrombin for 8 h and then treated with LMW-HA. ROS generation was detected by measuring H_2DCFDA fluorescence. Data are expressed in relative fluorescence units adjusted for protein concentration (mean ± S.E., $n = 4$, *, $p < 0.05$; **, $p < 0.001$). *B,* growth-arrested VSMC were treated with thrombin or LMW-HA or pretreated with thrombin for 8 h and then treated with LMW-HA. Rac1 activation in protein lysates containing equal amounts of protein was assessed using PAK-1 PBD pull-down assay. Western analysis of total Rac1 was used as an internal control for measuring Rac1 activity in lysates containing equal amounts of protein. Densitometric analysis of Rac1 activity, represented as fold-change in Rac1-GTP levels was calculated by first normalizing to total Rac1 levels in individual samples and then relative to untreated wild-type control (mean ± S.E., $n = 3$, *, $p < 0.01$; **, $p < 0.001$).

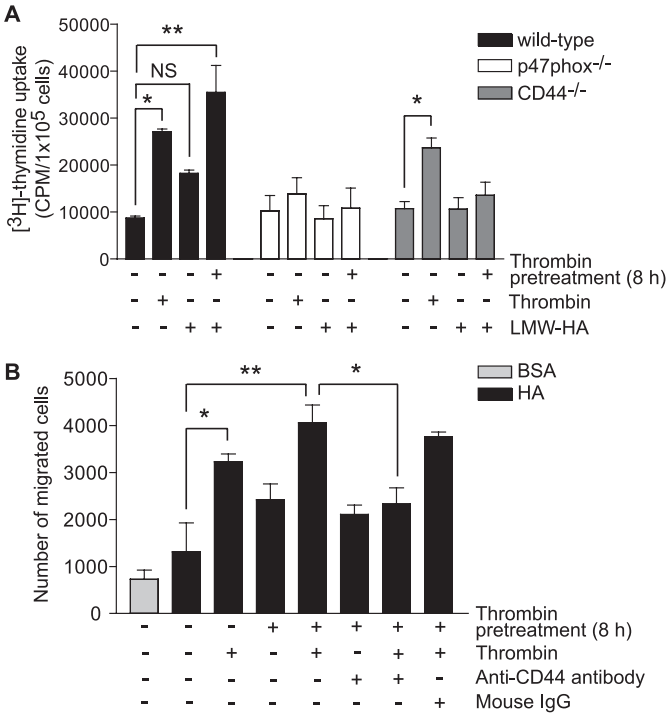

FIGURE 4. **LMW-HA enhances thrombin-induced VSMC proliferation and functional inhibition of CD44 attenuates thrombin-induced haptotactic migration of VSMC toward HMW-HA.** *A,* growth-arrested VSMC treated with thrombin or LMW-HA or pretreated with thrombin for 8 h and then treated with LMW-HA for 24 h. [^{3}H]Thymidine uptake was measured during the last 4 h of treatment. Data presented are mean ± S.E. ($n = 3$) and representative of three separate experiments (*, $p < 0.01$; **, $p < 0.001$; *NS*, not significant). *B,* haptotactic cell migration was measured using HMW-HA-coated transwell filters. VSMC were treated with thrombin or pretreated with thrombin for 8 h and then incubated with thrombin for 16 h. When antibody was used, VSMC were incubated with anti-CD44 IgG or normal mouse IgG at 1:100 dilution for 30 min before being seeded on the filters. Data presented are mean ± S.E. ($n = 3$) and representative of three separate experiments (*, $p < 0.05$; **, $p < 0.01$).

further enhanced in wild-type cells pretreated with thrombin for 8 h followed by treatment with LMW-HA, but not in CD44$^{-/-}$ VSMC. In contrast, none of these treatments significantly affected DHE fluorescence in p47$^{phox-/-}$ cells (data not shown).

Because both thrombin and HA are known to activate Rac1 GTPase (42, 43), a regulatory subunit of NADPH oxidase, we investigated the interaction of thrombin and LMW-HA on Rac1 activity by performing a PAK-1 PBD pulldown assay. Thrombin and LMW-HA increased Rac1 activity in wild-type cells by 80 and 70%, respectively ($p < 0.05$). Pretreatment with thrombin for 8 h prior to LMW-HA treatment increased Rac1 activity by 130% relative to untreated control ($p < 0.001$) and by 35% relative to LMW-HA treatment alone ($p < 0.05$) (Fig. 3*B*). Thrombin significantly increased Rac1 activity in CD44$^{-/-}$ VSMC ($p < 0.05$) (Fig. 3*B*), but LMW-HA or thrombin pretreatment followed by LMW-HA had no significant effect on Rac1 activity in CD44$^{-/-}$ VSMC. Thrombin, LMW-HA, or thrombin pretreatment followed by LMW-HA had no significant effect on the activation of Rac1 GTPase in p47$^{phox-/-}$ VSMC. Combined with our previous observations (4), these data suggest that NADPH oxidase is necessary for thrombin-induced CD44 expression and interaction of CD44 and HA, which in turn, activate NADPH oxidase.

LMW-HA Augments Thrombin-induced Proliferation of VSMC and CD44 Regulates Thrombin-induced Haptotactic Migration of VSMC toward HMW-HA—LMW-HA regulates VSMC proliferation in a CD44-dependent manner (6). To determine the role of ROS and confirm that of CD44 in LMW-HA-induced VSMC phenotype, we measured DNA synthesis in wild-type, p47$^{phox-/-}$, and CD44$^{-/-}$ cells treated with LMW-HA. LMW-HA increased DNA synthesis in wild-type VSMC, although the increase was not statistically significant (Fig. 4*A*). Treatment with LMW-HA had no effect in CD44$^{-/-}$ cells. Thrombin significantly increased DNA synthesis in wild-type and CD44 knock-out VSMC ($p < 0.01$) but not in p47$^{phox-/-}$ cells, consistent with our prior findings (28) (Fig. 4*A*). Thrombin pretreatment for 8 h prior to LMW-HA treatment increased [^{3}H]thymidine uptake in wild-type VSMC by 3.5-fold compared with untreated cells ($p < 0.001$) and by 2.2-fold compared with LMW-HA treatment alone ($p < 0.01$). LMW-HA or thrombin pretreatment followed by LMW-HA had no significant effect on DNA synthesis in p47$^{phox-/-}$ or CD44$^{-/-}$ cells. Together, these results indicate that interaction of LMW-HA with NADPH oxidase-dependent increased CD44 expression plays an important role in VSMC proliferation.

Because CD44 isoforms were known to enhance migration of melanoma cells on HA-coated surfaces (44, 45), we investigated whether CD44 regulates thrombin-induced migration of VSMC. In a haptotactic cell migration assay, a greater number of wild-type cells migrated toward HA as compared with bovine serum albumin. Treatment with thrombin significantly increased VSMC migration toward HA compared with untreated control ($p < 0.05$) (Fig. 4*B*). Thrombin pretreatment for 8 h followed by thrombin treatment further enhanced VSMC migration toward HA compared with thrombin treatment alone ($p < 0.05$). The migration of VSMC toward HA in response to thrombin alone and thrombin pretreatment + thrombin was significantly inhibited ($p < 0.05$) by anti-CD44 mAb, whereas isotype-matched mouse IgG had no inhibitory effect on the migration induced by thrombin pretreatment + thrombin treatment. Together with the published data (4), these CD44 functional inhibition studies indicate that thrombin-induced NADPH oxidase-dependent increased CD44 expression plays an important role in migration toward HA and LMW-HA-stimulated proliferation of VSMC.

NADPH Oxidase Regulates Expression of CD44 in the Aortas and HA in the Atherosclerotic Lesions—We previously reported lower levels of immunoreactive CD44 in atherosclerotic lesions in the aortas of apoE$^{-/-}$/p47$^{phox-/-}$ mice compared with apoE$^{-/-}$ mice, correlating with the decreased lesion size in apoE$^{-/-}$/p47$^{phox-/-}$ animals (4). Here, we compared the systemic expression of CD44 in protein lysates from aortas of apoE$^{-/-}$ and apoE$^{-/-}$/p47$^{phox-/-}$ mice fed a Western diet. The amount of CD44 in lysates from apoE$^{-/-}$ aortas was 2.6-fold higher than that from apoE$^{-/-}$/p47$^{phox-/-}$ animals ($p < 0.001$) (Fig. 5*A*) as measured by ELISA.

Because expression of CD44 and its interaction with HA are important determinants of the extent of atherosclerotic lesions in mice (6), we performed immunohistochemical analysis of HA expression in aortic sections of apoE$^{-/-}$ and apoE$^{-/-}$/p47$^{phox-/-}$ mice fed a Western diet. HA expression was significantly increased in apoE$^{-/-}$ aortic sections compared with those from apoE$^{-/-}$/p47$^{phox-/-}$ mice ($p < 0.05$) as detected by immunostaining using HA-binding protein, followed by histological scoring (Fig. 5, *B* and *C*). Intense HA expression was observed in the medial layer as confirmed by smooth muscle α-actin staining and in macrophage-enriched, oil red O positive areas of plaques (Fig. 5*B*).

These *in vivo* findings suggest that mechanisms similar to those observed in cultured VSMC for NADPH oxidase regulation of CD44 and HA expressions are important *in vivo*. Increased systemic expression of CD44 in apoE$^{-/-}$ aortas also indicates the role of NADPH oxidase in the induction of a pro-inflammatory milieu in mice.

Plasma Soluble CD44 and HA Levels Are Down-regulated in ApoE$^{-/-}$ Mice Deficient in p47^{phox} Subunit of NADPH Oxidase—Shedding and release of soluble CD44 into the systemic circulation is induced by various cytokines (46) and HA degradation and turnover are regulated by ROS, processes characteristic of an inflammatory response (18, 47). Furthermore, increased plasma HA levels have been associated with diabetic angiopathy and the susceptibility of diabetic patients to atherosclerosis (48, 49). Because the activation of NADPH oxidases

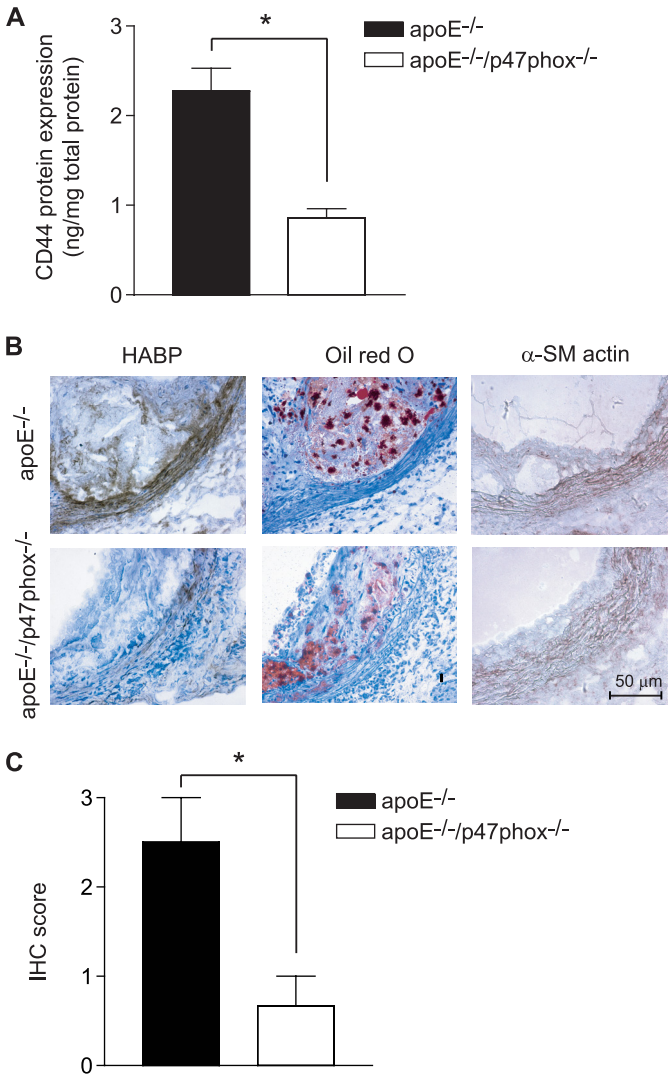

FIGURE 5. **CD44 expression is enhanced in aortas of apoE$^{-/-}$ mice, whereas HA expression was up-regulated in atherosclerotic lesions of apoE$^{-/-}$ mice as compared with apoE$^{-/-}$/p47$^{phox-/-}$ mice.** *A*, CD44 expression was measured in protein lysates from aortas of apoE$^{-/-}$ and apoE$^{-/-}$/p47$^{phox-/-}$ mice using CD44 ELISA. Data expressed are mean ± S.E. of five mice in each group (*, $p < 0.001$). *B*, representative aortic root sections from apoE$^{-/-}$ and apoE$^{-/-}$/p47$^{phox-/-}$ mice were stained using biotinylated HABP or oil red O. Localization of smooth muscle cell was shown by staining for α-SM actin. *C*, expression of HA in atherosclerotic lesions, determined by immunohistochemistry scoring. Data are mean ± S.E. ($n = 6$, *, $p < 0.05$).

contributes to inflammation (50, 51), we investigated soluble CD44 and HA levels in the plasma of apoE$^{-/-}$ and apoE$^{-/-}$/p47$^{phox-/-}$ mice on a Western diet. Soluble CD44 levels increased significantly in apoE$^{-/-}$ mice as compared with apoE$^{-/-}$/p47$^{phox-/-}$ and wild-type mice ($p < 0.05$) (Fig. 6*A*). Similarly, plasma HA levels in apoE$^{-/-}$/p47$^{phox-/-}$ mice were significantly lower than those in apoE$^{-/-}$ mice ($p < 0.01$) (Fig. 6*B*). There was no significant difference in either plasma-soluble CD44 or HA levels between wild-type and apoE$^{-/-}$/p47$^{phox-/-}$ mice. These data support our observation of increased expression of CD44 and HA in the aortic wall of apoE$^{-/-}$ mice. Furthermore, they suggest that increased NADPH oxidase-dependent degradation of HA and shedding and release of soluble CD44 antigen into systemic circulation

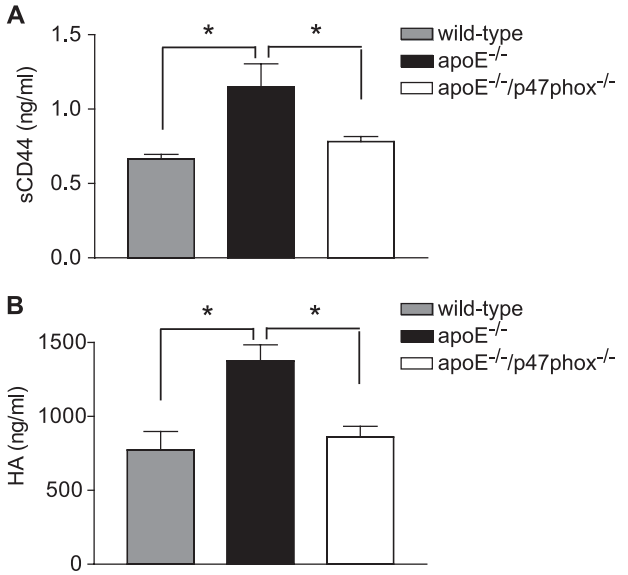

FIGURE 6. **HA and soluble CD44 concentrations are increased in the plasma of apoE$^{-/-}$ as compared with wild-type and apoE$^{-/-}$/p47$^{phox-/-}$ mice.** *A*, soluble CD44 concentration in the plasma of wild-type, apoE$^{-/-}$, and apoE$^{-/-}$/p47$^{phox-/-}$ mice was measured using a CD44 ELISA kit. Data expressed are mean ± S.E. of 12 mice in each group (*, $p < 0.05$). *B*, HA concentration in the plasma of wild-type, apoE$^{-/-}$, and apoE$^{-/-}$/p47$^{phox-/-}$ mice was measured using HA ELISA. Data expressed are mean ± S.E. of 10 mice in each group (*, $p < 0.01$).

enhance the inflammatory process and promote atherosclerosis in proatherogenic milieu.

CD44 and HA-dependent Gene Expression is Regulated in ApoE$^{-/-}$ Mice in a NADPH Oxidase-dependent Manner—Interaction of CD44 with LMW-HA results in the induction of chemokine gene expression in macrophages (36) and CD44 regulates vascular gene expression in atherosclerosis-prone regions of the vasculature (52). Soluble HA was shown to induce the expression of *Il1β*, *Tnfα*, and *Igf1* in bone-marrow derived macrophages (53) and *Ccl2*, *Ccl4*, and *Ccl5* in alveolar macrophages (36). We performed gene expression analysis of aortas from mice fed a Western diet to determine whether NADPH oxidase-dependent, increased expression of CD44 and HA will result in increased expression of the aforementioned genes in apoE$^{-/-}$ mice as compared with apoE$^{-/-}$/p47$^{phox-/-}$ mice. Real time RT-PCR analysis showed significantly higher levels of *Ccl2*, *Ccl5*, *Tnfα*, and *Igf1* expression in aortas of apoE$^{-/-}$ mice compared with the double knock-out mice ($p < 0.05$) (Table 1). Differences in the expression of *Ccl4* and *Il1β* trended to higher levels but were not significant. These results suggest that NADPH oxidase-dependent expression of CD44 and HA in the vascular wall and ROS-dependent HA degradation and release of LMW-HA leads to increased interaction of CD44 and LMW-HA and induction of pro-inflammatory cytokine expression in the vasculature and that this promotes atherogenesis.

Pharmacologic Inhibition of Nox1/Nox4-based NADPH Oxidase Attenuates Atherosclerosis, ROS Generation, Plasma 8-Isoprostane Levels, and CD44 and HA Expression in Atherosclerotic Lesions of ApoE$^{-/-}$ Mice—To confirm the role of NADPH oxidase in the regulation of CD44 and HA expression under pathophysiologic conditions, we tested the effect of

TABLE 1

Analysis of gene expression in aortas of apoE$^{-/-}$ *versus* apoE$^{-/-}$/p47$^{phox-/-}$ mice

Gene expression is based on real-time PCR analysis of RNA extracted from aortas ($n = 7$ for each genotype). Fold change calculated as expression in apoE$^{-/-}$ relative to apoE$^{-/-}$/p47$^{phox-/-}$ mice normalized to 18 S ribosomal RNA levels.

Gene	Accession number	ApoE$^{-/-}$ *vs* apoE$^{-/-}$/p47$^{phox-/-}$	*p* value
		Fold-change	
Ccl2 (monocyte chemotactic protein 1)	NM_011333	2.60	0.017
Ccl4 (macrophage inflammatory protein 1)	NM_013652	1.94	0.14
Ccl5 (regulated on activation, normal T-cell expressed and secreted)	NM_013653	4.90	0.027
Tnfα (tumor necrosis factor α)	NM_013693	4.12	0.026
Igf1 (insulin-like growth factor 1)	NM_010512	2.98	0.002
Il1β (interleukin 1β)	NM_008361	3.37	0.120

GKT136901 (Fig. 7*A*), a dual Nox1/Nox4 inhibitor, on atherosclerosis development in apoE$^{-/-}$ mice and the presence of CD44 and HA in atherosclerotic lesions. Nox4 regulates VSMC migration (3) and its expression is significantly enhanced in apoE$^{-/-}$ mice compared with wild-type mice (54). GKT136901 has a K_i in the range of 150–250 nM for human Nox1 and Nox4 (E_{max} of 90–100% at 33 μM) in a cell-free system and is bioavailable following oral administration.[4]

GKT136901 treatment significantly decreased the aortic atherosclerotic lesion area compared with vehicle treatment ($p < 0.05$) (Fig. 7*B*). There was no significant effect of GKT136901 on body weight, plasma total cholesterol, or triglyceride levels (Table 2). GKT136901 did significantly inhibit aortic ROS production as measured by the decrease in DHE fluorescence of fresh-frozen cross-sections ($p < 0.05$ *versus* vehicle) (Fig. 7*C*). To quantify systemic oxidative stress, plasma 8-isoprostane levels were determined using the Enzyme Immunoassay kit. A modest but significant decrease ($p < 0.05$) in plasma 8-isoprostane levels was observed in apoE$^{-/-}$ mice treated with GKT136901 compared with mice treated with the vehicle (Fig. 7*D*). Immunostaining of aortic cross-sections showed a significant decrease in CD44 and HA expression in atherosclerotic lesions of apoE$^{-/-}$ mice treated with GKT136901 compared with those from mice treated with the vehicle (Fig. 7, *E* and *F*). Furthermore, expression of monocyte/macrophage marker, CD11b, was significantly decreased in atherosclerotic lesions in mice treated with GKT136901 compared with the vehicle treatment (Fig. 7, *E* and *F*). These results support our *in vitro* data that NADPH oxidases regulate CD44 and HA expression and together with other published reports (4) indicate that CD44- and HA-dependent inflammatory cell recruitment and VSMC activation promotes atherosclerosis.

Thrombin Regulates HASMC CD44 and HA Expression in Nox1/Nox4-based NADPH Oxidase-dependent Manner—To determine whether CD44 and HAS2 are regulated in a similar manner in human vascular cells, we investigated thrombin-induced CD44 and HAS2 expression in HASMC. Western blot analysis revealed that thrombin regulates these proteins in a time-dependent manner, with peak CD44 expression at 4 h and

[4] C. Szyndralewiez and P. Page, unpublished data.

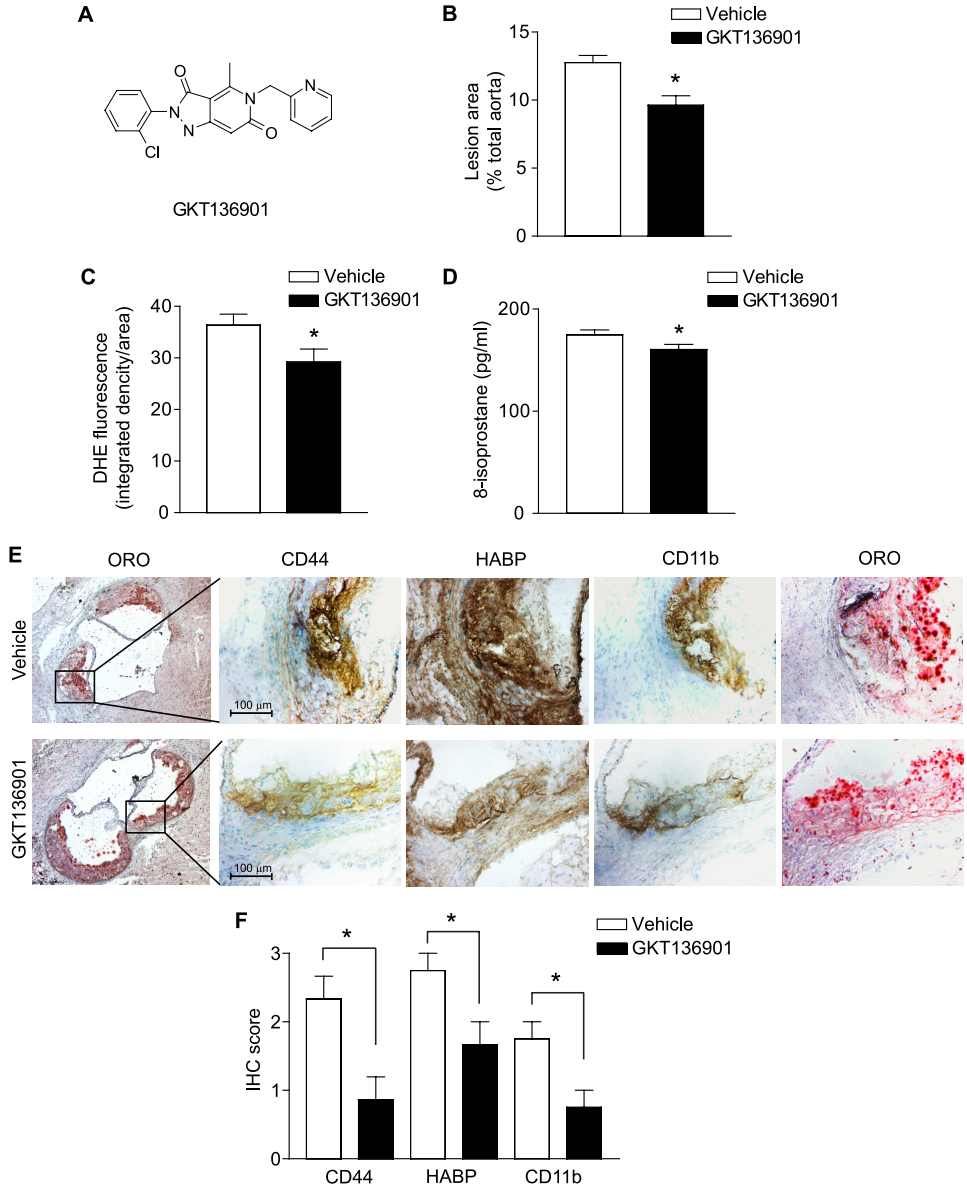

FIGURE 7. **Treatment with GKT136901, a pharmacologic inhibitor of Nox1/Nox4-based NADPH oxidases, decreases atherosclerosis, ROS generation, plasma 8-isoprostane levels, and CD44 and HA expression in atherosclerotic lesions in apoE$^{-/-}$ mice.** *A,* chemical structure of the selective Nox1/Nox4 inhibitor GKT136901. *B,* aortas from apoE$^{-/-}$ mice, fed a Western diet and treated with GKT136901 or vehicle, were fixed, stained with oil red O (*ORO*), and photographed. Oil red O-stained area was quantified as percent of whole aorta (mean ± S.E., $n = 15$, *, $p < 0.05$ *versus* vehicle). *C,* fresh frozen sections of aortic root were stained with DHE and fluorescence was detected using a confocal microscopy. Data are presented as integrated density relative to area (mean ± S.E., $n = 6$, *, $p < 0.05$). *D,* plasma 8-isoprostane levels were determined using the Enzyme Immunoassay kit (mean ± S.E., $n = 15$, *, $p < 0.05$). *E,* representative sections of aortic root stained for CD44, CD11b, HA, and with oil red O. *F,* expression of CD44, HA, and CD11b as determined by immunohistochemistry scoring (mean ± S.E., $n = 6$, *, $p < 0.05$).

HAS2 at 8 h (Fig. 8*A*). As an approach to determine the importance of NADPH oxidase in CD44 and HAS2 expression in HASMC, we treated cells with thrombin in the presence and absence of GKT136901. Pretreatment of HASMC with 30 μM GKT136901 for 1 h prior to thrombin treatment significantly inhibited intracellular ROS generation as measured by DCF fluorescence ($p < 0.01$) (Fig. 8*B*). GKT136901 also significantly inhibited thrombin-induced *Cd44* mRNA levels at 2 and 4 h ($p < 0.001$ and $p < 0.05$, respectively) and *Has2* mRNA levels at 2 h ($p < 0.01$) (Fig. 8, *C* and *D*) without significantly affecting *Nox1* or *Nox4* expression (data not shown). Consistent with this, GKT136901 abrogated any thrombin-induced increase in CD44 and HAS2 proteins levels (Fig. 8, *E* and *F*). Together with mouse cell culture and atherosclerosis model results, these data underline the relevance of ROS-sensitive regulation of CD44, HAS2, and HA expression in human atherosclerosis development.

DISCUSSION

The experiments reported here demonstrate that: 1) NADPH oxidase regulates thrombin induced CD44 expression via activation of AP-1; 2) increased synthesis and degradation of HA in thrombin-treated VSMC is regulated in NADPH oxidase-dependent manner; 3) LMW-HA enhances oxidative stress by activating Rac1 and subsequent induction of NADPH oxidase activity; 4) interaction of LMW-HA with NADPH oxidase-dependent increased CD44 expression in thrombin-treated VSMC plays a vital role in cell proliferation and migration; 5) CD44- and HA-dependent gene expression is significantly up-regulated in the aortas of apoE$^{-/-}$ mice compared with apoE$^{-/-}$/p47$^{phox-/-}$ mice; and 6) GKT136901, a pharmacological inhibitor of Nox1/Nox4-based NADPH oxidases not only inhibits oxidative stress, CD44 and HA expression, and atherosclerosis in apoE$^{-/-}$ mice, but also attenuates thrombin-induced ROS generation, CD44 and HA expression in HASMC. Together, these studies indicate that CD44 and HA constitute a Nox homologue-independent NADPH oxidase-regulated redox-sensitive signaling pathway active in the pathogenesis of atherosclerosis.

We and others have reported that CD44 expression is enhanced in response to arterial injury, inflammation, and atherosclerosis (4, 6, 33), interrelated pathologic processes that are regulated in a redox-sensitive manner (55). Our *in vitro* data that thrombin-stimulated CD44 expression is regulated by transcription factor AP-1 is consistent with the redox-sensitive regulation of this adhesion molecule and is in agreement with other reports (26, 33).

HA is synthesized in VSMC by three HA synthases (56), however, HAS2 is almost certainly the major HA synthesizing enzyme in VSMC based on two lines of evidence. First, when

TABLE 2

Body weight, plasma cholesterol, and triglycerides levels in apoE$^{-/-}$ mice fed a Western diet and treated with vehicle or GKT136901 (mean ± S.E., $n = 15$)

	Vehicle	GKT136901
Weight, g	31.88 ± 0.6176	32.05 ± 0.4134
Cholesterol, mg/dL	570.5 ± 67.39	603.0 ± 73.58
Triglycerides, mg/dL	37.20 ± 2.690	34.71 ± 3.200

Has2 is down-regulated using siRNA, VSMC proliferation is inhibited (23). Second, VSMC-specific overexpression of HAS2 enhances atherosclerosis in apoE$^{-/-}$ mice (20). Our data indicate that increased HAS2 expression and activity in response to thrombin treatment is dependent on NADPH oxidase activation. Furthermore, our data indicating that that NADPH oxidase regulates Hyal3 expression in VSMC treated with thrombin is significant because increased HA during pathological conditions is the sum of its synthesis and catabolism. This is also an interesting observation because Hyal3$^{-/-}$ mice do not exhibit any HA accumulation (57) and cellular overexpression of Hyal3 does not impart intrinsic hyaluronidase activity (58). In contrast, up-regulation of Hyal3 was reported in chondrocytes treated with cytokines (59). Although ROS can cleave HA in laboratory tests (17) and HA levels have been positively correlated with other oxidative stress makers in diabetic patients (47), evidence for the direct action of ROS on HA degradation in studies using cell culture or cell-free extracts is absent.

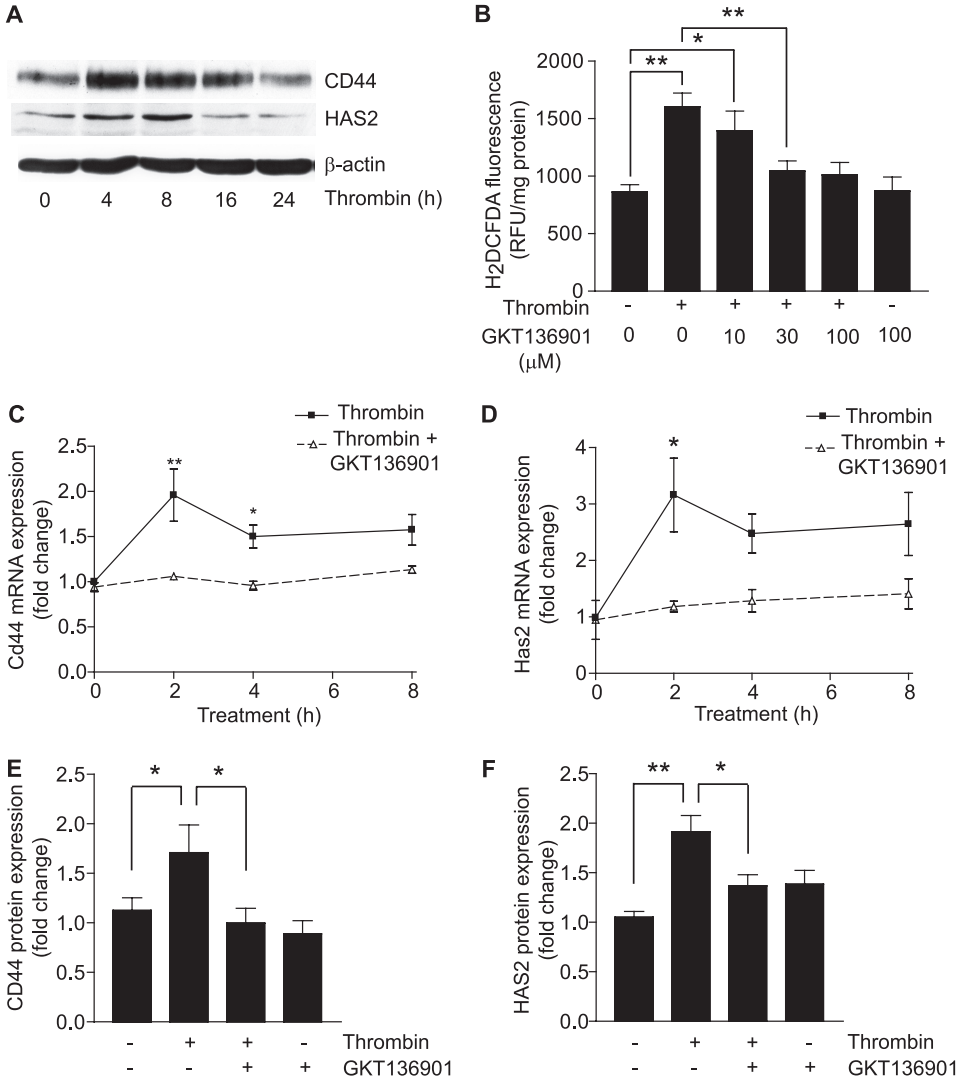

FIGURE 8. **GKT136901 inhibits thrombin-induced CD44 and HAS2 expression in HASMC.** *A*, growth-arrested HASMC were treated with thrombin for the indicated times. Expression of CD44 and HAS2 was determined by Western blot analysis. *B*, HASMC were treated with thrombin or pretreated with various concentrations of GKT136901 and then treated with thrombin. ROS generation was detected by measuring H_2DCFDA fluorescence. Data are expressed in relative fluorescence units adjusted for protein concentration (mean ± S.E., $n = 4$, *, $p < 0.05$; **, $p < 0.01$). *C*, real time RT-PCR analysis of *Cd44* RNA expression in HASMC treated with thrombin alone or thrombin and GKT136901 for the indicated times. Data represent fold-change in gene expression, normalized to 18 S RNA, and relative to untreated wild-type control (mean ± S.E., $n = 3$, *, $p < 0.05$; **, $p < 0.001$). *D*, real time RT-PCR analysis of *Has2* RNA expression in cells treated with thrombin alone or thrombin and GKT136901 for the indicated times. Data are expressed as fold-change in gene expression, normalized to 18 S RNA, and relative to untreated wild-type control (mean ± S.E., $n = 3$, *, $p < 0.01$). *E*, Western blot analysis of CD44 protein levels in HASMC after an 8-h treatment with thrombin or GKT136901 alone or GKT136901 and thrombin together. Densitometric analysis of CD44 protein levels, represented as fold-change, was calculated by first normalizing to β-actin levels in individual samples and then relative to untreated control (mean ± S.E., $n = 3$, *, $p < 0.05$). *F*, Western blot analysis of HAS2 protein levels in HASMC after an 8-h treatment with thrombin or GKT136901 alone or GKT136901 and thrombin together. Densitometric analysis of HAS2 protein levels, represented as fold-change, was calculated by first normalizing to β-actin levels in individual samples and then relative to untreated control (mean ± S.E., $n = 3$, *, $p < 0.05$; **, $p < 0.01$).

The increase in thrombin-induced NADPH oxidase activity by LMW-HA may be due to either enhanced Rac1 activity (Fig. 3*B*) or enhanced CD44 expression caused by thrombin pretreatment, or both. HA has been reported to induce ROS production in a CD44-dependent manner (43, 60) and NADPH oxidase mediates the increase in ROS production as down-regulation of p47^{phox}, p67^{phox}, or Rac1 decreased ROS levels (43). Arterial injury and atherosclerotic lesions are characterized by enhanced thrombin expression and activity (40, 41) and increased ROS production in the arteries of apoE$^{-/-}$ *versus* apoE$^{-/-}$/p47$^{phox-/-}$ mice (29) may result from the interaction of increased thrombin and HA levels. NADPH oxidase activation increases HA synthesis and LMW-HA enhances NADPH oxidase activity suggesting a positive feedback loop between HA and NADPH oxidase activation.

Increased VSMC migration and proliferation are important events in the development of atherosclerosis and restenosis. Wild-type VSMC

proliferate more rapidly than p47$^{phox-/-}$ VSMC in the presence of thrombin and LMW-HA, indicating that NADPH oxidase activation and subsequent synthesis of CD44 are major contributors of VSMC mitogenesis likely *in vivo* under pathophysiological conditions. The importance of NADPH oxidase-dependent CD44 expression in atherogenesis is supported by our finding that thrombin-induced haptotactic migration of VSMC is significantly decreased in the presence of monoclonal anti-CD44 antibody.

The increase in CD44 expression observed in the current investigation in the aortas of apoE$^{-/-}$ mice (compared with those in apoE$^{-/-}$/p47$^{phox-/-}$ mice) together with the observation of Cuff *et al.* (6) that CD44$^{-/-}$/apoE$^{-/-}$ mice develop significantly decreased atherosclerosis (again compared with apoE$^{-/-}$ littermates) indicates that NADPH oxidases and CD44 play a critical role in atherogenesis. The increase in plasma sCD44 levels in apoE$^{-/-}$ mice compared with wild-type and apoE$^{-/-}$/p47$^{phox-/-}$ mice further indicates that activation of NADPH oxidase in proatherogenic milieu releases sCD44 by proteolytic cleavage of membrane-anchored CD44. This may well be from the stimulation of matrix metalloproteinases (61, 62). Our *in vivo* data showing increased HA expression in medial VSMC of atherosclerotic lesions in apoE$^{-/-}$ mice compared with apoE$^{-/-}$/p47$^{phox-/-}$ mice supports our cell culture data of decreased HA levels in p47$^{phox-/-}$ VSMC compared with wild-type in response to thrombin treatment. These findings are consistent with the observation of Chai *et al.* (20) that overexpression of HA in aortic VSMC of apoE$^{-/-}$ mice increases atherosclerosis. Interestingly, apoE$^{-/-}$ mice had higher plasma HA levels than wild-type and apoE$^{-/-}$/p47$^{phox-/-}$ mice consistent with increased HA degradation under proatherogenic conditions.

In addition to their role in VSMC proliferation and migration, CD44 and HA participate in many processes that promote atherogenesis. For example, CD44 contributes to the initial rolling interaction between lymphocytes and endothelium and once within the subendothelial space, CD44 mediates interactions between leukocytes, VSMC, and parenchymal cells (19). In this context it is noteworthy that pharmacologic inhibition of Nox1/Nox4-based NADPH oxidase in apoE$^{-/-}$ mice not only attenuated ROS generation in the aortic wall and plasma 8-isoprostane levels but also decreased atherosclerotic burden, CD44 and HA levels in the aortic wall and macrophage recruitment into these lesions (Fig. 7). To our knowledge, this is the first study to show that a specific inhibitor of Nox1/Nox4 activity significantly decrease atherosclerosis in apoE$^{-/-}$ mice. This inhibitor may have therapeutic potential as it inhibited CD44 and HA expression and oxidative stress in HASMC. Increased HA levels in medial VSMC were correlated with increased mechanical stiffness and strength of the aortas, which is linked to endothelial dysfunction and atherogenesis (20, 63). Because HA interacts with lipoproteins through hydrophobic interactions (64), increased HA might promote atherogenesis by retaining lipoproteins in the arterial wall.

Finally, our analysis of known HA-regulated genes (36, 53) in the aortas of apoE$^{-/-}$ and apoE$^{-/-}$/p47$^{phox-/-}$ mice demonstrated a NADPH oxidase-dependent regulation of *Ccl2* (*Mcp1*), *Ccl5* (*RANTES*), *Tnfα*, and *Igf1*. MCP-1 plays an important role in the recruitment of monocytes/macrophages to vascular lesions. Localized overexpression of MCP-1 in the vessel wall, in the backdrop of hypercholesterolemia, induces early atherosclerotic lesions in rabbits (65) and increased expression of serum MCP-1 was observed in hypertensive patients with diffuse atherosclerosis as well (66). In concurrence with our results, Bae *et al.* (67) have recently reported that RANTES is regulated in a NADPH oxidase-dependent manner. Furthermore, a transient increase in RANTES levels was reported in patients experiencing unstable angina pectoris (68). TNF-α plays a key role in the inflammatory cascade associated with atherosclerosis (69) and several studies support the association of increased TNF-α levels with increased risk of myocardial infarction (70, 71). The role of IGF-1 in atherogenesis is controversial. Several studies suggest that IGF-1 accelerates atherogenesis (72, 73), whereas another study has reported an association of low serum IGF-1 levels with increased risk for ischemic heart disease (74). Our data indicating pharmacologic inhibition of Nox1/Nox4-based NADPH oxidase markedly decreases CD44 and HA expression in the vascular wall validates our hypothesis that NADPH oxidase activation promotes atherosclerosis via CD44- and HA-dependent processes.

In summary, our data provide insight into the molecular mechanisms by which NADPH oxidase activation promotes atherosclerotic lesion formation. NADPH oxidases mediate agonist-induced HA synthesis by regulating both HA synthetic and degradation enzymes and a positive feedback loop between HA and NADPH oxidase increases oxidative stress and enhances atherosclerosis. Interaction between increased CD44 and HA levels resulting from NADPH oxidase activation in hyperlipidemic background induces chemokine, cytokine, and growth factor production, which promote atherosclerosis. Specific inhibitors of NADPH oxidase function may provide an effective therapy for treating atherosclerosis not just by decreasing oxidative burden but also by attenuating the molecular pathways that promote atherosclerosis.

REFERENCES

1. Bedard, K., and Krause, K. H. (2007) *Physiol. Rev.* **87,** 245–313
2. Hilenski, L. L., Clempus, R. E., Quinn, M. T., Lambeth, J. D., and Griendling, K. K. (2004) *Arterioscler. Thromb. Vasc. Biol.* **24,** 677–683
3. Lyle, A. N., Deshpande, N. N., Taniyama, Y., Seidel-Rogol, B., Pounkova, L., Du, P., Papaharalambus, C., Lassègue, B., and Griendling, K. K. (2009) *Circ. Res.* **105,** 249–259
4. Vendrov, A. E., Madamanchi, N. R., Hakim, Z. S., Rojas, M., and Runge, M. S. (2006) *Circ. Res.* **98,** 1254–1263
5. Ponta, H., Sherman, L., and Herrlich, P. A. (2003) *Nat. Rev. Mol. Cell Biol.* **4,** 33–45
6. Cuff, C. A., Kothapalli, D., Azonobi, I., Chun, S., Zhang, Y., Belkin, R., Yeh, C., Secreto, A., Assoian, R. K., Rader, D. J., and Puré, E. (2001) *J. Clin. Invest.* **108,** 1031–1040
7. Krettek, A., Sukhova, G. K., Schönbeck, U., and Libby, P. (2004) *Am. J. Pathol.* **165,** 1571–1581
8. Hägg, D., Sjöberg, S., Hultén, L. M., Fagerberg, B., Wiklund, O., Rosengren, A., Carlsson, L. M., Borén, J., Svensson, P. A., and Krettek, A. (2007) *Atherosclerosis* **190,** 291–297
9. Jain, M., He, Q., Lee, W. S., Kashiki, S., Foster, L. C., Tsai, J. C., Lee, M. E., and Haber, E. (1996) *J. Clin. Invest.* **97,** 596–603
10. Okamoto, I., Tsuiki, H., Kenyon, L. C., Godwin, A. K., Emlet, D. R., Holgado-Madruga, M., Lanham, I. S., Joynes, C. J., Vo, K. T., Guha, A., Matsumoto, M., Ushio, Y., Saya, H., and Wong, A. J. (2002) *Am. J. Pathol.* **160,** 441–447
11. Mayer, S., zur Hausen, A., Watermann, D. O., Stamm, S., Jäger, M., Gitsch,

G., and Stickeler, E. (2008) *J. Cancer Res. Clin. Oncol.* **134,** 1229–1235
12. Sjöberg, S., Fogelstrand, L., Hulthe, J., Fagerberg, B., and Krettek, A. (2005) *Metabolism* **54,** 139–141
13. Stern, R., Asari, A. A., and Sugahara, K. N. (2006) *Eur. J. Cell Biol.* **85,** 699–715
14. Toole, B. P., Wight, T. N., and Tammi, M. I. (2002) *J. Biol. Chem.* **277,** 4593–4596
15. Philipson, L. H., Westley, J., and Schwartz, N. B. (1985) *Biochemistry* **24,** 7899–7906
16. Evanko, S. P., Johnson, P. Y., Braun, K. R., Underhill, C. B., Dudhia, J., and Wight, T. N. (2001) *Arch. Biochem. Biophys.* **394,** 29–38
17. Harada, H., and Takahashi, M. (2007) *J. Biol. Chem.* **282,** 5597–5607
18. McNeil, J. D., Wiebkin, O. W., Betts, W. H., and Cleland, L. G. (1985) *Ann. Rheum. Dis.* **44,** 780–789
19. Puré, E., and Cuff, C. A. (2001) *Trends Mol. Med.* **7,** 213–221
20. Chai, S., Chai, Q., Danielsen, C. C., Hjorth, P., Nyengaard, J. R., Ledet, T., Yamaguchi, Y., Rasmussen, L. M., and Wogensen, L. (2005) *Circ. Res.* **96,** 583–591
21. Riessen, R., Wight, T. N., Pastore, C., Henley, C., and Isner, J. M. (1996) *Circulation* **93,** 1141–1147
22. Kolodgie, F. D., Burke, A. P., Farb, A., Weber, D. K., Kutys, R., Wight, T. N., and Virmani, R. (2002) *Arterioscler. Thromb. Vasc. Biol.* **22,** 1642–1648
23. van den Boom, M., Sarbia, M., von Wnuck Lipinski, K., Mann, P., Meyer-Kirchrath, J., Rauch, B. H., Grabitz, K., Levkau, B., Schrör, K., and Fischer, J. W. (2006) *Circ. Res.* **98,** 36–44
24. Miyazaki, T., Yomota, C., and Okada, S. (2001) *Polymer Degradation and Stability* **74,** 77–85
25. Page, P., Orchard, M., Fioraso-Cartier, L., and Mottironi, B. (2008) *Pyrazolo Pyridine Derivatives as NADPH Oxidase Inhibitors*, WO 2008=113856 A1, GenKyoTex
26. Mishra, J. P., Mishra, S., Gee, K., and Kumar, A. (2005) *J. Biol. Chem.* **280,** 26825–26837
27. Moon, S. K., Thompson, L. J., Madamanchi, N., Ballinger, S., Papaconstantinou, J., Horaist, C., Runge, M. S., and Patterson, C. (2001) *Am. J. Physiol. Heart Circ. Physiol.* **280,** H2779–H2788
28. Madamanchi, N. R., Li, S., Patterson, C., and Runge, M. S. (2001) *J. Biol. Chem.* **276,** 18915–18924
29. Barry-Lane, P. A., Patterson, C., van der Merwe, M., Hu, Z., Holland, S. M., Yeh, E. T., and Runge, M. S. (2001) *J. Clin. Invest.* **108,** 1513–1522
30. Pfaffl, M. W., Horgan, G. W., and Dempfle, L. (2002) *Nucleic Acids Res.* **30,** e36
31. Stuhlmeier, K. M. (2005) *J. Immunol.* **174,** 7376–7382
32. Tchivilev, I., Madamanchi, N. R., Vendrov, A. E., Niu, X. L., and Runge, M. S. (2008) *J. Biol. Chem.* **283,** 22193–22205
33. Foster, L. C., Wiesel, P., Huggins, G. S., Pañares, R., Chin, M. T., Pellacani, A., and Perrella, M. A. (2000) *FASEB J.* **14,** 368–378
34. Rao, G. N., Katki, K. A., Madamanchi, N. R., Wu, Y., and Birrer, M. J. (1999) *J. Biol. Chem.* **274,** 6003–6010
35. Hodge-Dufour, J., Noble, P. W., Horton, M. R., Bao, C., Wysoka, M., Burdick, M. D., Strieter, R. M., Trinchieri, G., and Puré, E. (1997) *J. Immunol.* **159,** 2492–2500
36. McKee, C. M., Penno, M. B., Cowman, M., Burdick, M. D., Strieter, R. M., Bao, C., and Noble, P. W. (1996) *J. Clin. Invest.* **98,** 2403–2413
37. McKee, C. M., Lowenstein, C. J., Horton, M. R., Wu, J., Bao, C., Chin, B. Y., Choi, A. M., and Noble, P. W. (1997) *J. Biol. Chem.* **272,** 8013–8018
38. Camenisch, T. D., Spicer, A. P., Brehm-Gibson, T., Biesterfeldt, J., Augustine, M. L., Calabro, A., Jr., Kubalak, S., Klewer, S. E., and McDonald, J. A. (2000) *J. Clin. Invest.* **106,** 349–360
39. Noble, P. W. (2002) *Matrix Biol.* **21,** 25–29
40. Walters, T. K., Gorog, D. A., and Wood, R. F. (1994) *J. Vasc. Res.* **31,** 173–177
41. Westmuckett, A. D., Lupu, C., Goulding, D. A., Das, S., Kakkar, V. V., and Lupu, F. (2000) *Thromb. Haemost.* **84,** 904–911
42. Diebold, I., Djordjevic, T., Petry, A., Hatzelmann, A., Tenor, H., Hess, J., and Görlach, A. (2009) *Circ. Res.* **104,** 1169–1177
43. Kim, Y., Lee, Y. S., Choe, J., Lee, H., Kim, Y. M., and Jeoung, D. (2008) *J. Biol. Chem.* **283,** 22513–22528
44. Thomas, L., Byers, H. R., Vink, J., and Stamenkovic, I. (1992) *J. Cell Biol.* **118,** 971–977
45. Yoshinari, C., Mizusawa, N., Byers, H. R., and Akasaka, T. (1999) *Melanoma Res.* **9,** 223–231
46. Cichy, J., Kulig, P., and Puré, E. (2005) *Biochim. Biophys. Acta* **1745,** 59–64
47. Gao, F., Koenitzer, J. R., Tobolewski, J. M., Jiang, D., Liang, J., Noble, P. W., and Oury, T. D. (2008) *J. Biol. Chem.* **283,** 6058–6066
48. Mine, S., Okada, Y., Kawahara, C., Tabata, T., and Tanaka, Y. (2006) *Endocr. J.* **53,** 761–766
49. Nieuwdorp, M., Holleman, F., de Groot, E., Vink, H., Gort, J., Kontush, A., Chapman, M. J., Hutten, B. A., Brouwer, C. B., Hoekstra, J. B., Kastelein, J. J., and Stroes, E. S. (2007) *Diabetologia* **50,** 1288–1293
50. Wei, Y., Whaley-Connell, A. T., Chen, K., Habibi, J., Uptergrove, G. M., Clark, S. E., Stump, C. S., Ferrario, C. M., and Sowers, J. R. (2007) *Hypertension* **50,** 384–391
51. Basuroy, S., Bhattacharya, S., Leffler, C. W., and Parfenova, H. (2009) *Am. J. Physiol. Cell Physiol.* **296,** C422–C432
52. Zhao, L., Hall, J. A., Levenkova, N., Lee, E., Middleton, M. K., Zukas, A. M., Rader, D. J., Rux, J. J., and Puré, E. (2007) *Arterioscler. Thromb. Vasc. Biol.* **27,** 886–892
53. Noble, P. W., Lake, F. R., Henson, P. M., and Riches, D. W. (1993) *J. Clin. Invest.* **91,** 2368–2377
54. Xu, X., Gao, X., Potter, B. J., Cao, J. M., and Zhang, C. (2007) *Arterioscler. Thromb. Vasc. Biol.* **27,** 871–877
55. Ali, Z. A., Bursill, C. A., Douglas, G., McNeill, E., Papaspyridonos, M., Tatham, A. L., Bendall, J. K., Akhtar, A. M., Alp, N. J., Greaves, D. R., and Channon, K. M. (2008) *Circulation.* **118,** Suppl. 14, S71–S77
56. Fischer, J. W., and Schrör, K. (2007) *Thromb. Haemost.* **98,** 287–295
57. Atmuri, V., Martin, D. C., Hemming, R., Gutsol, A., Byers, S., Sahebjam, S., Thliveris, J. A., Mort, J. S., Carmona, E., Anderson, J. E., Dakshinamurti, S., and Triggs-Raine, B. (2008) *Matrix Biol.* **27,** 653–660
58. Hemming, R., Martin, D. C., Slominski, E., Nagy, J. I., Halayko, A. J., Pind, S., and Triggs-Raine, B. (2008) *Glycobiology* **18,** 280–289
59. Flannery, C. R., Little, C. B., Hughes, C. E., and Caterson, B. (1998) *Biochem. Biophys. Res. Commun.* **251,** 824–829
60. Basoni, C., Reuzeau, E., Croft, D., Génot, E., and Kramer, I. M. (2006) *Biochem. Biophys. Res. Commun.* **343,** 609–616
61. Inoue, N., Takeshita, S., Gao, D., Ishida, T., Kawashima, S., Akita, H., Tawa, R., Sakurai, H., and Yokoyama, M. (2001) *Atherosclerosis* **155,** 45–52
62. Deem, T. L., and Cook-Mills, J. M. (2004) *Blood* **104,** 2385–2393
63. Peng, X., Haldar, S., Deshpande, S., Irani, K., and Kass, D. A. (2003) *Hypertension* **41,** 378–381
64. Srinivasan, S. R., Yost, K., Radhakrishnamurthy, B., Dalferes, E. R., Jr., and Berenson, G. S. (1980) *Atherosclerosis* **36,** 25–37
65. Namiki, M., Kawashima, S., Yamashita, T., Ozaki, M., Hirase, T., Ishida, T., Inoue, N., Hirata, K., Matsukawa, A., Morishita, R., Kaneda, Y., and Yokoyama, M. (2002) *Arterioscler. Thromb. Vasc. Biol.* **22,** 115–120
66. Tucci, M., Quatraro, C., Frassanito, M. A., and Silvestris, F. (2006) *J. Hypertens.* **24,** 1307–1318
67. Bae, Y. S., Lee, J. H., Choi, S. H., Kim, S., Almazan, F., Witztum, J. L., and Miller, Y. I. (2009) *Circ. Res.* **104,** 210–218
68. Kraaijeveld, A. O., de Jager, S. C., de Jager, W. J., Prakken, B. J., McColl, S. R., Haspels, I., Putter, H., van Berkel, T. J., Nagelkerken, L., Jukema, J. W., and Biessen, E. A. (2007) *Circulation* **116,** 1931–1941
69. Hansson, G. K. (2001) *Arterioscler. Thromb. Vasc. Biol.* **21,** 1876–1890
70. Cesari, M., Penninx, B. W., Newman, A. B., Kritchevsky, S. B., Nicklas, B. J., Sutton-Tyrrell, K., Rubin, S. M., Ding, J., Simonsick, E. M., Harris, T. B., and Pahor, M. (2003) *Circulation* **108,** 2317–2322
71. Bennet, A. M., van Maarle, M. C., Hallqvist, J., Morgenstern, R., Frostegård, J., Wiman, B., Prince, J. A., and de Faire, U. (2006) *Atherosclerosis* **187,** 408–414
72. Kawachi, S., Takeda, N., Sasaki, A., Kokubo, Y., Takami, K., Sarui, H., Hayashi, M., Yamakita, N., and Yasuda, K. (2005) *Arterioscler. Thromb. Vasc. Biol.* **25,** 617–621
73. Colao, A., Spiezia, S., Di Somma, C., Pivonello, R., Marzullo, P., Rota, F., Musella, T., Auriemma, R. S., De Martino, M. C., and Lombardi, G. (2005) *J. Endocrinol. Invest.* **28,** 440–448
74. Juul, A., Scheike, T., Davidsen, M., Gyllenborg, J., and Jørgensen, T. (2002) *Circulation* **106,** 939–944